BMC Genomics

RESEARCH

Open Access

Post-transcriptional regulation in early cell fate commitment of germ layers

Rubens Gomes-Júnior[1†], Cintia Delai da Silva Horinouchi[1†], Aruana Fagundes Fiuza Hansel-Fröse[1], Annanda Lyra Ribeiro[1], Isabela Tiemy Pereira[1], Lucia Spangenberg[2,3] and Bruno Dallagiovanna[1*]

Abstract

Background Cell differentiation during development is orchestrated by precisely coordinated gene expression programs. While some regulatory mechanisms are well understood, there is a significant room to explore unresolved aspects of lineage choice and cell-fate decisions, as many events in these processes are still not fully elucidated. Given that, gene expression is influenced not only by transcriptional control but also by post-transcriptional events. Here, we described the presence of post-transcriptional regulation on gene expression during lineage commitment across all three embryonic germ layers. We employed monolayer differentiation protocols to map early transcriptional and post-transcriptional events in human embryonic stem cell specification. This approach included obtaining representative populations from the three germ layers, followed by sequencing of both polysome-bound and total RNAs.

Results We characterized our model by its unique expression profile and the presence of specific markers for each differentiation. RNA sequencing revealed a consistent pattern of gene upregulated and downregulated when comparing the transcriptome and translatome during the differentiation of all three germ layers. By comparing these datasets, we identified genes subjected to post-transcriptional regulation in all germ layer differentiations and categorized the nature of this regulation. GO analysis demonstrated that polysome profiling serves as a complementary technique, capturing nuances that may be overlooked when analyzing only the transcriptome. Finally, we directly compared the transcriptome and translatome to identify genes actively recruited to the translation machinery, uncovering unique features specific to each germ layer.

Conclusions Substantial post-transcriptional modulation was found during germ layer commitment, emphasizing the translatome potency in capturing nuanced gene expression regulation. These findings highlight the post-transcriptional regulation's critical role in early embryonic development, offering new insights into the molecular mechanisms of cell differentiation.

Keywords Post-transcriptional regulation, Polysome profiling, Embryology, Germ layer, Human development

[†]Rubens Gomes-Júnior and Cintia Delai da Silva Horinouchi contributed equally to this work.

*Correspondence:
Bruno Dallagiovanna
bruno.dallagiovanna@fiocruz.br
Full list of author information is available at the end of the article

Introduction

Since the beginning of the twentieth century, Experimental Embryology has tried to describe how an organism is built up in terms of cellular changes, interactions, and communication. In the last decades, Genetics and Molecular Biology allowed the modeling of embryonic development revealing the molecular mechanisms involved in cell fate and tissue designation and composition [1]. Due to ethical issues, the usage of human early embryos in studies for elucidation of developmental processes is made difficult. Instead, human pluripotent stem cells, like embryonic stem cells (hESC) lineages have been shown to be an efficient tool to study early development events [2]. hESC can be induced to differentiate in vitro into cells of all three embryonic germ layers mimicking human development and allowing the assessment of the key mechanisms implicated in early cell fate commitment [3].

Lineage choice and cell-fate decisions are modulated by highly coordinated gene expression programs which allow the expression of lineage-specific genes while repressing unsuitable genes for that lineage [4]. Robust gene expression analysis, therefore, enables the elucidation of transcriptional mechanisms and epigenetic events involved in the phenomena of cell fate commitment. It's known that the modulation of a complex and dynamic pluripotency circuit is driven by a series of specific transcription factors and epigenetic regulators which are sufficient to hold the cells in a pluripotent state [5]. However, how the cells leave pluripotency and which mechanisms are involved in the lineage choice is not clear and researchers are trying to elucidate the phenomenon of early lineage commitment by different approaches and methodologies [6–8]. Most of the applied strategies primarily emphasize transcriptional analysis, however, it is widely recognized that gene expression regulation extends beyond transcriptional control and is also modulated by post-transcriptional events. Protein expression is significantly influenced by these translational events [9].

Few studies explored the early lineage commitment process at the post-transcriptional level [10–12]. In a previous study from our group, a strong post-transcriptional regulation (PTR) was found to occur during the mesoderm commitment of hESC [13]. These results aroused the interest to understand whether this phenomenon of PTR is restricted to mesodermal differentiation or common to the process of lineage choice across all three embryonic germ layers.

Here, monolayer differentiation protocols were employed to obtain representative populations of the three germ layers to delineate early transcriptional and post-transcriptional events during hESC specification. Subsequently, polysome-bound and total RNAs were sequenced. Our results show a significant presence of post-transcriptional modulation during germ layers commitment. Furthermore, we highlighted the reliability of the translatome in capturing nuances, revealing a unique pattern in gene expression regulation. These findings reinforce the crucial role of PTR in early embryonic development, opening new perspectives to understand the molecular mechanisms of cell differentiation.

Methods

Cell culture and induction of germ layers differentiation

Human embryonic stem cell, H1 line, was obtained from WiCell Research Institute (Madison, WI, USA) under a Materials Transfer Agreement (No. 18-W0416) with Carlos Chagas Institute. The H1 hESC line is derived from a male and exhibits a regular karyotype. Cells were cultured on Matrigel-coated dishes using mTeSR-1 medium (Stem Cell Technologies). The medium was replaced daily until cells reached 70–80% confluence. Cells were maintained in a 37 °C, 5% CO_2 incubator.

For endoderm differentiation, the cells were subjected to a protocol adapted from Caruso and coworkers [14]. The cells were seeded at 5×10^4 cells/cm^2 in a 24-wells plate pre-coated with Geltrex hESC-qualified (Thermo Fisher Scientific) in StemFlex medium (Thermo Fisher Scientific) with 10 µM Y27632 (Med Chem Express). After 24 h, the medium was replaced to remove the ROCK inhibitor. On the following day (D0), the medium was changed to RPMI 1640 (Gibco) supplemented with 1% l-glutamine, 1% non-essential amino acids and 2% B-27 minus insulin (Gibco). Induction was initiated by adding 3 µM CHIR99021 (TOCRIS) and 50 ng/ml of Activin A (B&D systems) during the medium replacement. After 2 days (D2), the medium was replaced to the base medium containing only 50 ng/ml Activin A (B&D systems). On day 4 (D4), cells were collected for RNA isolation.

For neuroectodermal differentiation, the cells were subjected to a protocol adapted from Yan and coworkers [15]. The cells were seeded at 2.5×10^4 cells/cm^2 in a 6-wells plate pre-coated with Geltrex hESC-qualified (Thermo Fisher Scientific) in StemFlex medium (Thermo Fisher Scientific) with 10 µM Y27632 (Med Chem Express). The next day (D0), the medium was changed to Neural Induction Medium (Thermo Fisher Scientific) containing 2% Neural Induction Supplement (Thermo Fisher Scientific). Following the manufacturer´s instructions, the medium was changed on days 3, 5, and 7. On D8, cells were collected for RNA isolation.

For mesoderm differentiation, the cells were subjected to a protocol adapted from Lian and coworkers [16]. The cells were seeded at 10^5 cells/cm^2 in a Geltrex-precoated 24-well plate in StemFlex medium (Thermo Fisher

Scientific) with 10 μM Y27632 (Med Chem Express). In the next two days the medium was daily replaced until the culture reached 100% confluence. The monolayer was induced to mesoderm differentiation in RPMI 1640 (Gibco) supplemented with 2% B27 minus insulin (Gibco) and 12 μM CHIR99021 (TOCRIS). After 24 h of induction, cells were collected for RNA isolation.

Polysome profiling

Polysome profiling was performed as previously described [17]. Cells at undifferentiated and differentiated stages were treated with 0.1 mg/mL cycloheximide for 10 min or 10 mg/mL puromycin for 1 h at 37 °C. After incubation, cells were detached and lysed in polysome lysis buffer (15 mM Tris HCl, pH 7.4, 15 mM $MgCl_2$, 0.3 M NaCl, 1% Triton X-100, 40 U/μL RNAse Out, 50 U/μL DNAse). Lysis was performed for 10 min on ice, then centrifuged at 12.000×g for 10 min at 4 °C. For both cycloheximide and puromycin treatments, supernatants were loaded on 10–50% sucrose gradients (BioComp model 108 Gradient Master v.5.3) and centrifuged (SW40 rotor, HIMAC CP80WX HITACHI) at 270.000×*g* for 120 min at 4 °C.

Sucrose gradient fractions were isolated using the ISCO gradient fractionation system (ISCO Model 160 Gradient Former Foxy Jr. Fraction Collector) coupled to a UV light for RNA detection, which recorded the polysome profiling at 254 nm. A typical polysome gradient profile displays a pattern of peaks corresponding to various known RNA ribosomes complexes. Fractions were identified based on the peak distribution observed in the RNA detection chart, then polysome fractions were pooled and added to an equal volume of TRIreagent (Thermo Fisher Scientific). Total RNA and polysome fractions RNA were isolated by Direct-zol™ RNA kit (Zymo® Research), following the manufacturer's instructions.

RNA-seq and data analysis

Total and polysome RNA-seq was performed using H1 hESC cell line in undifferentiated and germ layer differentiated states. Quality assessment and trimming of reads was done with FastQC and Trim Galore (v.0.4.0) [18]. Reads were mapped to hg38/GRCh38 with HISAT2 (v.2.1.0) [19] and counted with HTSeq 174 (v.0.11.1) [20]. Significantly differentially expressed genes were calculated with DESeq2 175 (v.1.24.0) [21] with an adjusted *p*-value cutoff of 0.01 and $\log_2$FoldChange cutoff of 2. Gene Ontology (GO) analysis was performed using enrichR [22]. Venn diagram was performed using FunRich (v.3.1.3) [23]. RNA-seq data are available at NCBI Sequence Read Archive, accessing number PRJNA1144790. Heatmaps were generated with heatmap.2 function from the gplots package (v. 3.1.3.1), based on genes that passed an adjusted *p*-value cutoff of ≤ 0.05. Hierarchical clustering of selected genes was performed on both row and column using stats package (v. 4.4.1) from base R, with scaling applied by rows and dendrograms reordered accordingly. Gene set enrichment analysis (GSEA) was performed using GSEA Desktop (v. 4.3.3). Gene sets were ranked based on a combined metric calculated as the product of the log2 fold change (log2FC) and the -log10 of the adjusted *p*-value (-log10(p-adj)). Enrichment plots were generated using the Molecular Signature Database for Biological Processes with the GSEA software.

cDNA synthesis and qPCR

cDNA synthesis was performed using Improm-II Reverse Transcription System (Promega), following the manufacturer's instructions. For polysomal samples, a GFP spike-in (5 pg) was included in each reaction. Quantitative PCR reactions were performed with GoTaq® qPCR Master Mix (Promega). Analyses were carried out in QuantStudio™ 5 Real-Time PCR System. GFP detection was used for normalization in these samples. The primers are listed in Supplementary Table 1.

Data and statistical analysis

Graphed data are expressed as mean ± SD. Statistical analysis was performed with Prism 8.0 software (GraphPad Software). For comparisons between two mean values the student's unpaired t-test was performed. A *p*-value lower than 0.05 was considered statistically significant.

Results

Transcriptome and translatome: similar distribution with different gene profiles

To evaluate PTR during germ layer differentiation, we induced a human embryonic stem cell (hESC) line to independently differentiate into endoderm, mesoderm or neuroectoderm. Polysome profiling was performed to access transcripts under translation process, and polysome-bound RNAs were collected. In parallel, total RNA was isolated from the same samples. Both polysome-bound and total RNA were submitted to RNA-sequencing (Fig. 1A). Polysome-profiling analysis did not detect changes in the polysome fraction between the germ layers, except for a slight decrease of RNA in endoderm samples, suggesting that polysome recruitment is less prominent in endodermal cells. We also observed an increase of RNA in the monosome fraction for the neuroectoderm samples compared to the other two differentiated cell types, further supporting the differences in translational activity among the germ layers (Figure S1A). Initially, we evaluated the identity of polysome-bound

(translatome) and total RNA (transcriptome) sets of transcripts. Principal component analysis and heatmap of gene expression profile revealed distinct clustering of each germ layer in both the transcriptome and translatome, indicating a unique set of expressed genes for each differentiation pathway (Figure S1 B-D). When the transcriptome was compared to the translatome within the same germ layer, we observed distinctly clustered for transcriptome and translatome samples, except for one sample in the endoderm where the difference is more subtle (Figure S1 E). This data suggests that the transcriptome and the translatome in this experimental model have distinct sets of representative genes.

To validate our differentiation datasets, we analyzed the expression profile of each differentiation condition by heatmap using genes with p-adjusted ≤ 0.05 at least one differentiation comparing with undifferentiated state. We confirmed the identity of each sample (Fig. 1B). Additionally, we verified the expression of specific marker genes for each germ layer, based on their well-established roles as key markers of germ layer specification in the literature. Most of them are transcription factors, such as TBXT, TBX6, GATA4, EOMES, SOX17, PAX8, NEUROD1 and HOXA2 [24–29], confirming the success of the differentiation process (Fig. 1C).

Lastly, we performed a gene set enrichment analysis (GSEA) by comparing our dataset with the Molecular Signature Database (MSigDB) for biological processes (Fig. 1D). In the endoderm samples, we observed a positive enrichment score for terms such as "Digestive Tract Morphogenesis", "Glandular Epithelial Cell Differentiation", and "Pancreas Development", all of which are associated with tissues derived from this germ layer. In the mesoderm samples, we identified positive enrichment for "Mesoderm Morphogenesis", "Somite Development", and "Mesoderm Development" indicating that mesoderm has an early phenotype comparing with endoderm and neuroectoderm dataset. In the neuroectoderm samples, we found enrichment for terms like "Embryonic Skeletal System Development", "Midbrain Development", and "Ear Development", confirming the commitment of these samples to ectoderm-derived cell types. Interestingly, across all three germ layers, we observed a positive enrichment score for at least one early developmental biological process, such as "Gastrulation", "Embryo Development", and "Cell Fate Specification", indicating that the cells, while committed to their respective germ layers, remain partially undifferentiated. Collectively, the results confirm the successful differentiation of the three germ layers.

Next, we aimed to identify the genes that were regulated during the three distinct differentiation protocols in each transcriptome and translatome dataset. For this, we identified the difference in expression profile of each differentiation to the undifferentiated cells. Upon analyzing the differentially expressed genes (DEG), a gene was considered differentially expressed if it exhibited a fold change (log2) ≥ |1.5| and an adjusted *p*-value ≤ 0.05 relative to hESC. We observed a similarity in the distribution of DEGs between the transcriptome and translatome across the three groups compared to the pluripotent state, with slightly fewer DEGs in mesoderm samples (Fig. 2A). In both total RNA and polysome samples, we assessed gene expression profiles after germ layer commitment. For total RNA, we identified 4,846 DEGs in endoderm, being almost 51% up-regulated and 49% down-regulated. In mesoderm, we found 2,254 DEGs, with 32% up-regulated and 67% down-regulated. Lastly, for neuroectoderm, we found 5,958 DEGs, with 56% up-regulated and 43% down-regulated. In parallel, polysome fraction analysis revealed 5,977 DEGs in endoderm, with a similar proportion to total RNA showing 53% up-regulated and almost 47% down-regulated genes. The same pattern was observed during the differentiation of the other two embryonic germ layers. For mesoderm and neuroectoderm, we found 2,592 and 5,722 DEGs, respectively, in the polysome fraction. In polysome samples of mesoderm, 42% of the DEGs were up-regulated and 58% were down-regulated, while in neuroectoderm, 35% were up-regulated and 65% were down-regulated. The proportion of DEGs being up- and down-regulated was similar when comparing transcriptome and translatome data in endoderm samples, however, in mesoderm we detected an increase about 10% of up-regulated genes in translatome. Interestingly, the opposite of mesoderm was observed in the neuroectoderm, in this translatome data we detected a decrease of DEGs being up-regulating compared to the transcriptome. In addition, we analyzed

(See figure on next page.)

Fig. 1 Characterization of germ layer differentiation in hESCs. **A** Overview of the experimental design. hESCs are represented in magenta; hESC-derived endoderm, mesoderm, and neuroectoderm cells are depicted in brown, green, and purple, respectively. **B** Heatmap showing the expression profile (adjusted *p*-value ≤ 0.05) in each differentiation condition. Values are presented as normalized read counts. The color key legend is displayed above the chart. **C** Heatmap of differentiation markers expression. Values are presented as normalized read counts. Gene names are listed on the right. The color key legend is displayed above the chart. **D** Gene set enrichment analysis (GSEA) of up-regulated DEGs in total RNA for each differentiation condition. The four enrichment plots were arbitrarily selected from the top twenty gene enrichment results

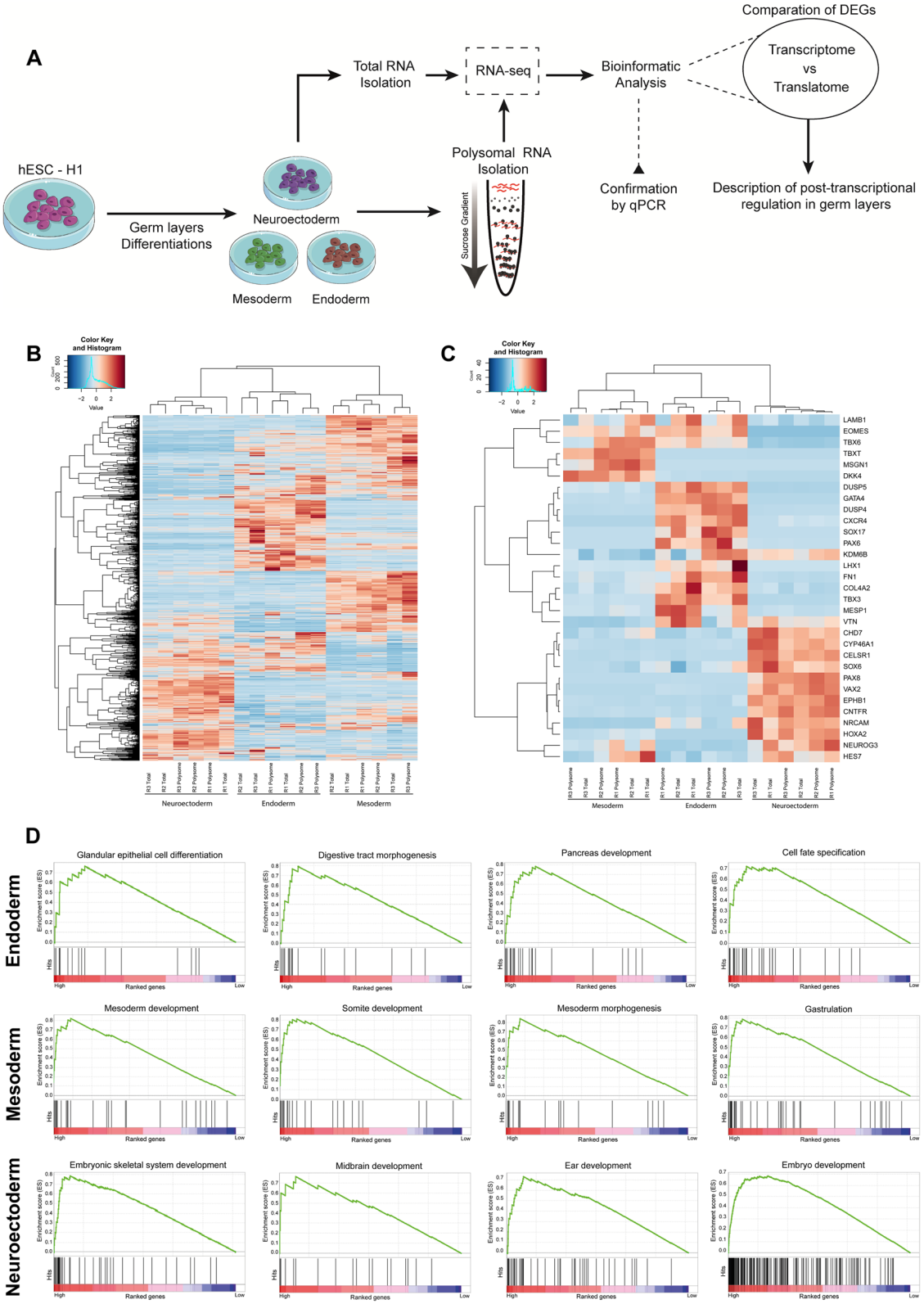

Fig. 1 (See legend on previous page.)

the gene biotype of the up- or down-regulated genes in transcriptome and translatome (Fig. 2B). Surprisingly, we found a high percentage of lncRNA in both transcriptome and translatome, with a similar distribution. Additionally, as expected, the majority of DEGs in our analysis were categorized as protein coding.

To validate the efficiency of our technique in isolating polysome-bound RNA, we selected three genes identified in the translatome of the neuroectoderm from the polysome data. Therefore, we performed polysome profiling after treatment with puromycin, which disassembles polysomes, and compared it to polysome profiling under normal conditions with cycloheximide, which stabilizes RNA associated with ribosomal complexes (polysomes). The genes were subsequently analyzed by qPCR. The disassembly of polysomes was verified by measuring absorbance at 254 nm (Fig. S2A-B), where a decrease in RNA detection in the polysome fractions was observed post-puromycin treatment. qPCR analysis further confirmed that the genes identified by RNA-seq were indeed associated with the translation machinery (Fig. S2C).

Post-transcriptional regulation is present during the differentiation process of all three germ layers

Although translatome and transcriptome exhibited a similar distribution of up- and down-regulated genes, we identified a distinct set of DEGs between them, suggesting the potential involvement of PTR. To investigate the occurrence of PTR, we then examined genes that exhibited differential expression patterns in the transcriptome and translatome data compared to the undifferentiated cells. To categorize the type of regulation, we used the classification described in Pereira et al., 2019. It is considered "Coordinate" regulation when the genes were up- or down-regulated similarly in both polysome fraction and total RNA. RNAs that were up-regulated in polysome fraction but showed no change in total RNA (up-loaded), or that were non-differentially expressed (non-DEG) in polysome but were down-regulated in total RNA (down-buffered), we considered, in both cases, as "post-transcriptional positive" regulation. On the contrary, RNAs that were down-regulated in polysome fraction but showed no change in total RNA (down-loaded), or genes that were non-DEG in polysome but were up-regulated in total RNA (up-buffered), we considered, in both cases, as "post-transcriptional negative" regulation (Table 1). To avoid categorizing narrowly up- or down-regulated genes as non-DEGs, we applied a criterion requiring genes to exhibit a fold-change $\leq|1|$ to be considered non-DEGs.

Analyzing the distribution of genes within the categories, we observed both positive and negative post-transcriptional modulation across all embryonic germ layer groups (Fig. 3A). We identified genes that, despite being up- or down-regulated in transcriptome, were not recruited to the polysome RNA (green dots), indicating buffered regulation during differentiation. Conversely, we also observed cases where genes were non-DEG in total RNA but showed fluctuations in their recruitment to the translation machinery (yellow dots), suggesting a loaded effect. When assessing the number of genes undergoing changes in polysome recruitment, as expected, we found that the majority of genes recruited to the polysome were coordinated with an increase in the transcriptome for all three germ layers, however, we found a substantial number of genes post-transcriptionally regulated. In the endoderm, post-transcriptional positive regulation (PTPR) was observed in 447 genes under an up-loaded effect and 230 genes under a down-buffered effect, while for post-transcriptional negative regulation (PTNR), we identified 343 and 34 genes under down-loaded and up-buffered effects, respectively (Fig. 3B). Similarly, we found both positive and negative regulations in the other two germ layers. For the mesoderm, we identified 143 and 64 genes under up-loaded and down-buffered effects, respectively, for PTPR, while 26 genes were down-loaded and only 1 gene was up-buffered during PTNR. The same pattern was observed in the neuroectoderm, where 207 genes were up-loaded and 85 were down-buffered in PTPR, while 206 genes were down-loaded and 21 genes were up-buffered in PTNR.

Analyzing the percentage of PTR across all DEGs identified during germ layer differentiation, we observed that, while both positive and negative regulation were present, the up-buffering category was the least prominent across all germ layers. Overall, in negative regulation, endoderm exhibited 9.02% of up-buffered and 90.98%

(See figure on next page.)

Fig. 2 Characterization of differentially expressed genes during differentiation into germ layers. **A** Volcano plots for each differentiation protocol display data for the Total (transcriptome) and Polysome (translatome) fractions separately. The threshold in axis Y indicates adjusted *p*-value = 0.05 and in axis X indicates log2 fold change = |1.5|. Blue dots represent down-regulated genes, while red dots indicate up-regulated genes compared to pluripotent hESCs. The charts on the right represent the percentage of up- and down-regulated genes among the identified DEGs. The percentage of total DEGs is provided to each fraction. The number of total DEGs (log2FC ≥|1.5|; adjusted *p*-value ≤ 0.05) is shown below each chart. **B** Identification of the gene biotypes of the DEGs. The proportion of protein coding genes, lncRNA and other types among the Up- and Down-regulated DEGs in the three cell commitments. Absolute numbers are shown below the percentage. Color key legends are present below the charts

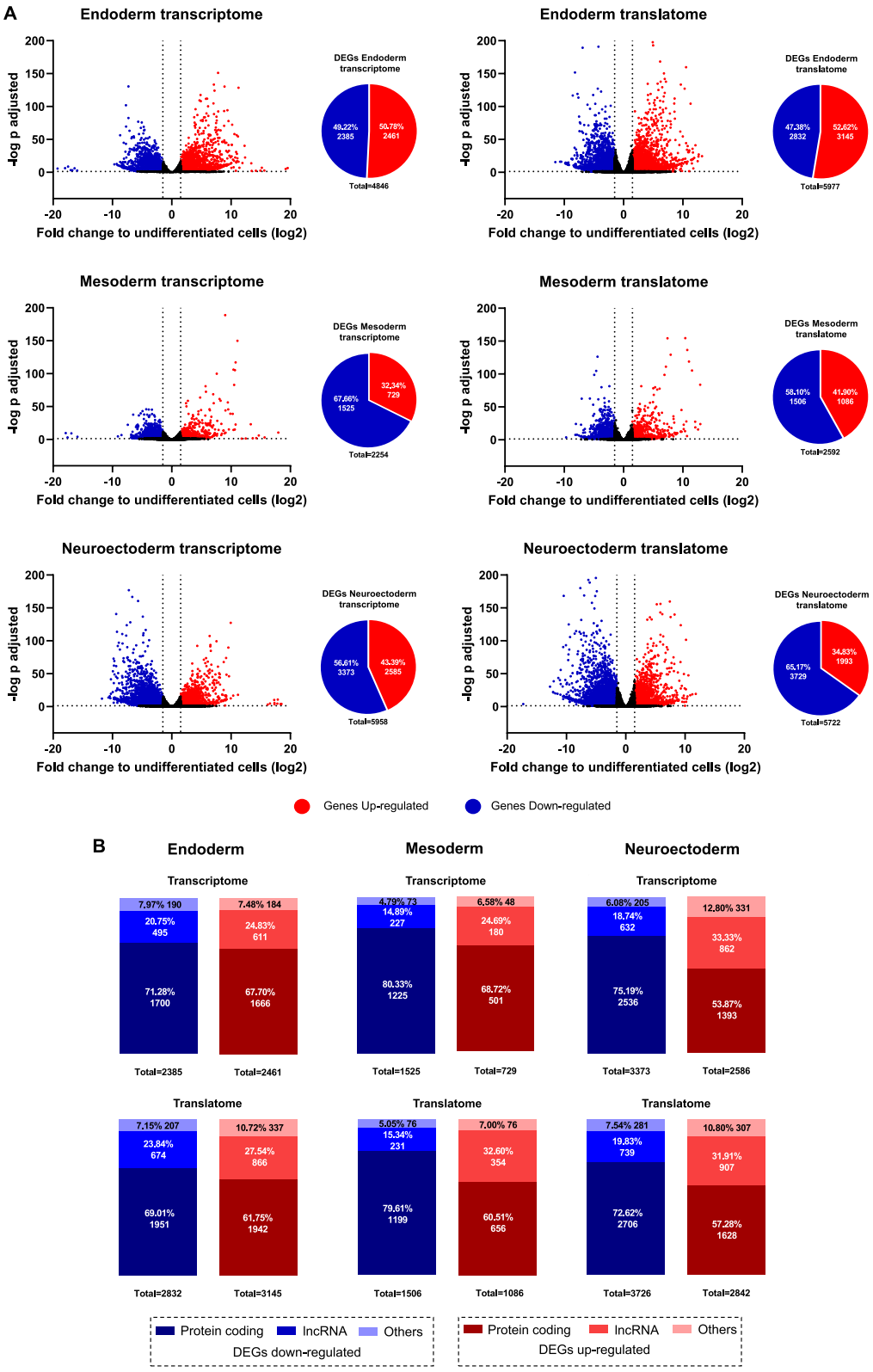

Fig. 2 (See legend on previous page.)

Table 1 Categorization of post-transcriptional regulation based on gene expression. Adapted from Pereira et al., 2019

Total	Polysome	Category	Regulation	Final Expression
↑	↑	Up coordinate	Coordinate	Positive
↓	↓	Down coordinate		Negative
-	↑	Up-loaded	Post-transcriptional positive	Positive
↓	-	Down-buffered		
-	↓	Down-loaded	Post-transcriptional negative	Negative
↑	-	Up-buffered		

Red arrows indicate up-regulated genes, blue arrows indicate down-regulated genes, dashes indicate non-DEG

of down-loaded. For mesoderm and neuroectoderm, we found 3.70% and 96.30% of up-buffer effect, and 90.75% and 9.25% of down-loaded, respectively. In positive regulation, for endoderm we found 33.97% being down-buffered and 66.03% being up-loaded. For mesoderm and neuroectoderm, we found 30.42% and 29.11% of down-buffer effect, and 69.08% and 70.89% of up-loaded respectively (Fig. 3C). In addition to the observed differences between negative and positive PTR, these findings suggest that PTR plays a role in early embryonic differentiation. Notably, the mesoderm exhibited the lowest number of DEGs subject to PTR, whereas the endoderm displayed the highest number of DEGs under PTR. However, the proportion of genes regulated by PTR was similar across all germ layers. The lists of PTR-regulated genes are provided in Additional Tables 1–3.

Translatome and transcriptome are complementary in certain types of analysis

To evaluate the accuracy of transcriptome and translatome data in capturing nuances during differentiation processes, we performed a Gene Ontology (GO) analysis of Biological Processes on the gene sets from each group. Differences were observed between the analyses of total RNA and polysome-associated RNA (Fig. 4A). For the mesoderm and endoderm, we ranked the GO terms using a combined score from EnrichR, which is calculated by taking the log of the *p*-value from Fisher's exact test and multiplying it by the z-score of deviation from the expected rank. This approach was used due to the biological similarities between these two germ layers.

In the endoderm group, the term "Endoderm Formation" (GO:0001706) was exclusive to the polysome set, while the term "Endoderm Development" (GO:0007492) ranked higher in the polysome set compared to the total set. For the mesoderm, no significant differences were observed between the two data sets. Genes contributing to the main pathways in this process, such as WNT signaling (GO:2,000,096; GO:2,000,095), were identified in the analyses of both data set. However, some embryogenic processes like anterior/posterior axis and pattern specification are present in polysome dataset.

In the neuroectoderm, the term "Nervous System Development" (GO:0007399) was present in both total and polysome data sets. Interestingly, the number of contributing genes increased from 78 in the total set to 93 in the polysome set. On the other hand, some differentiation-related terms, such as "Central Nervous System Development" (GO:0007417), was top-ranked in the polysome set. Conversely, terms like "Kidney Development" (GO:0001822) and "Eye Development" (GO:0001654) were found in the total set. These results indicate that transcriptome and translatome data highlight different biological processes during differentiation.

We also analyzed down-regulated DEGs (Fig. 4B), where more pronounced differences between polysome and total RNA data sets were detected. While some overlapping terms, such as "Regulation of Endothelial Cell Chemotaxis to Fibroblast Growth Factor" (GO:2,000,544) in the endoderm or "Potassium Ion Transmembrane Transport" (GO:0071805) in the neuroectoderm, were found in both data sets, polysome and total sets have a unique top-ranked terms.

Finally, we compared up- and down-regulated DEGs common to all three germ layers (Figure S3). Similar lists of terms were identified between the transcriptome and translatome, with slight differences in the number of contributing genes in the polysome set. This analysis highlights the potential to detect distinct biological processes by comparing transcriptome and translatome data. In some cases, such as in the neuroectoderm, these datasets can complement each other, providing a more comprehensive understanding of differentiation processes.

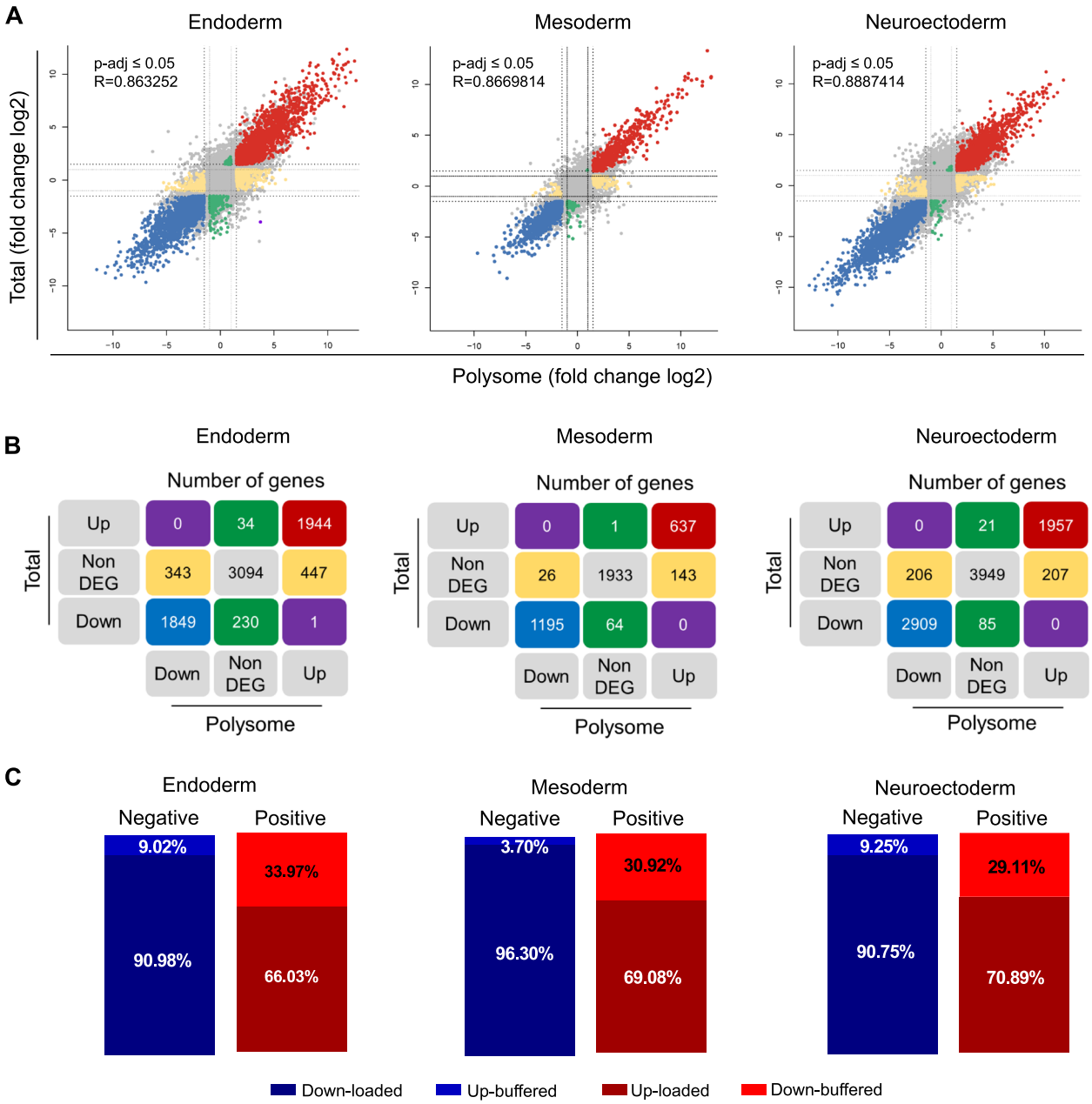

Fig. 3 Post-transcriptional regulation in each germ layer. **A** Scatterplot showing the genes using fold change (log2) of Total and Polysome fraction. Threshold in both axis X and Y indicate value of |1.5| and |1| marked as dotted line. Adjusted *p*-value of DEGs and correlation coefficient are shown above the charts. Red and blue dots represent genes with coordinate regulation being up- and down-regulated respectively. Green dots represent genes differentially expressed exclusively in total RNA. Yellow dots represent genes differentially expressed exclusively in polysome-bound RNA. Purple dots represent genes with opposite expression pattern in total RNA and polysome-bound RNA. Grey dots represent genes with adjusted *p*-value > 0.05. **B** Table showing the number of genes present in total and polysome fraction comparing the categories of DEGs (log2FC ≥|1.5|; adjusted *p*-value ≤ 0.05). The colors of each square are the same as the previous scatterplot. **C** Proportion of genes in each regulation category separated by negative and positive regulation for the three germ layers. Category legend is below the charts

Direct comparison of the transcriptome and translatome reveals unique patterns across the germ layers

Finally, we compared the transcriptome and translatome for each germ layer after the differentiation. This direct comparison allowed us to identify whether specific genes are actively recruited to or depleted from the translation machinery. However, this analysis focuses exclusively on the differentiated state, potentially overlooking whether

A

Biological Process	p-value	Genes
Endoderm Formation (GO:0001706)	3.04E-09	19/35
Cardiac Right Ventricle Morphogenesis (GO:0003215)	1.70E-05	8/12
Endoderm Development (GO:0007492)	7.51E-06	9/14
Cardiac Atrium Morphogenesis (GO:0003209)	1.41E-06	11/18
Coronary Vasculature Development (GO:0060976)	4.90E-04	5/7

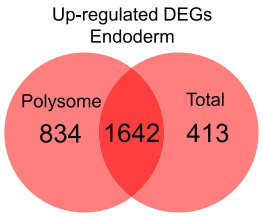

Biological Process	p-value	Genes
His-Purkinje System Development (GO:0003164)	5.10E-04	4/5
Positive Regulation Of Wnt Signaling Pathway, Planar Cell Polarity Pathway (GO:2000096)	5.10E-04	4/5
Endochondral Bone Morphogenesis (GO:0060350)	4.15E-06	8/12
Endoderm Development (GO:0007492)	1.55E-06	8/14
Coronary Vasculature Development (GO:0060976)	2.00E-04	5/7

Biological Process	p-value	Genes
Mammary Gland Epithelial Cell Differentiation (GO:0060644)	1.07E-04	4/7
Positive Regulation Of Wnt Signaling Pathway, Planar Cell Polarity Pathway (GO:2000096)	7.40E-04	3/5
Anterior/Posterior Axis Specification (GO:0009948)	8.91E-07	8/20
Anterior/Posterior Pattern Specification (GO:0009952)	2.50E-10	17/59
Regulation Of Wnt Signaling Pathway, Planar Cell Polarity Pathway (GO:2000095)	2.06E-04	4/8

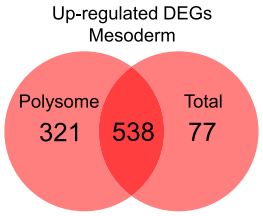

Biological Process	p-value	Genes
Positive Regulation Of Wnt Signaling Pathway, Planar Cell Polarity Pathway (GO:2000096)	2.76E-04	3/5
Mammary Gland Epithelial Cell Differentiation (GO:0060644)	2.88E-05	4/7
Regulation Of Wnt Signaling Pathway, Planar Cell Polarity Pathway (GO:2000095)	5.62E-05	4/8
Type B Pancreatic Cell Development (GO:0003323)	5.40E-04	3/6
Negative Regulation Of Steroid Metabolic Process (GO:0045939)	5.40E-04	3/6

Biological Process	p-value	Genes
Nervous System Development (GO:0007399)	6.22E-11	93/433
Cilium Movement (GO:0003341)	7.63E-11	26/59
Central Nervous System Development (GO:0007417)	1.05E-07	61/283
Cilium Assembly (GO:0060271)	1.97E-07	54/243
Cilium Organization (GO:0044782)	3.44E-07	51/228

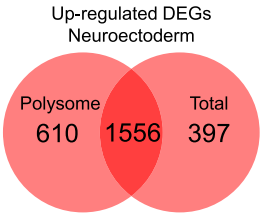

Biological Process	p-value	Genes
Cilium Movement (GO:0003341)	9.57E-13	27/59
Nervous System Development (GO:0007399)	7.20E-08	78/433
Kidney Development (GO:0001822)	2.44E-06	21/71
Eye Development (GO:0001654)	5.94E-06	18/58
Anterior/Posterior Pattern Specification (GO:0009952)	7.78E-06	18/59

B

Biological Process	p-value	Genes
Pyrimidine Nucleobase Catabolic Process (GO:0006208)	1.71E-05	6/7
Nucleobase Catabolic Process (GO:0046113)	1.25E-04	5/6
Regulation Of Endothelial Cell Chemotaxis To Fibroblast Growth Factor (GO:2000544)	1.25E-04	5/6
Postsynaptic Membrane Assembly (GO:0097104)	3.94E-04	5/7
Detection Of Stimulus Involved In Sensory Perception Of Pain (GO:0062149)	0.002404	4/6

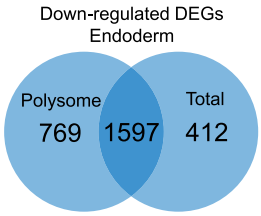

Biological Process	p-value	Genes
Regulation Of Postsynaptic Neurotransmitter Receptor Activity (GO:0098962)	6.55E-05	6/9
Membrane Depolarization During Action Potential (GO:0086010)	8.28E-06	8/13
Regulation Of Catecholamine Secretion (GO:0050433)	5.77E-08	14/27
Calcium Ion-Regulated Exocytosis Of Neurotransmitter (GO:0048791)	1.76E-05	8/14
Regulation Of Endothelial Cell Chemotaxis To Fibroblast Growth Factor (GO:2000544)	0.001289	4/6

Biological Process	p-value	Genes
Phospholipase C-activating Dopamine Receptor Signaling Pathway (GO:0060158)	2.74E-04	4/6
Response To Alkaloid (GO:0043279)	2.74E-04	4/6
Potassium Ion Transport (GO:0006813)	1.46E-11	32/122
Adenylate Cyclase-Activating Dopamine Receptor Signaling Pathway (GO:0007191)	0.002738	3/5
Glomerulus Vasculature Development (GO:0072012)	0.002738	3/5

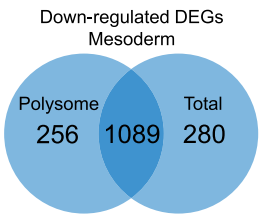

Biological Process	p-value	Genes
Detection Of Stimulus Involved In Sensory Perception Of Pain (GO:0062149)	8.45E-06	5/6
Sodium-Dependent Phosphate Transport (GO:0044341)	6.47E-04	4/7
Behavioral Fear Response (GO:0001662)	0.002882	3/5
Epithelial Tube Formation (GO:0072175)	0.002882	3/5
Equilibrioception (GO:0050957)	0.002882	3/5

Biological Process	p-value	Genes
Potassium Ion Transmembrane Transport (GO:0071805)	1.17E-09	51/137
Potassium Ion Transport (GO:0006813)	1.40E-09	47/122
Chemical Synaptic Transmission (GO:0007268)	3.90E-07	76/273
Monoatomic Cation Transmembrane Transport (GO:0098655)	6.50E-07	77/281
Adenylate Cyclase-Modulating G Protein-Coupled Receptor Signaling Pathway (GO:0007188)	7.54E-07	51/163

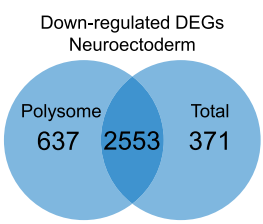

Biological Process	p-value	Genes
Chemical Synaptic Transmission (GO:0007268)	81/273	81/273
Anterograde Trans-Synaptic Signaling (GO:0098916)	59/199	59/199
Monoatomic Cation Transmembrane Transport (GO:0098655)	75/281	75/281
Potassium Ion Transport (GO:0006813)	41/122	41/122
Potassium Ion Transmembrane Transport (GO:0071805)	44/137	44/137

Fig. 4 Gene ontology analysis of up- and down-regulated genes. **A** Gene ontology using the up-regulated genes (log2FC ≥ 1.5; adjusted *p*-value ≤ 0.05) comparing polysome and total genes sets for each differentiation. **B** Gene ontology using the down-regulated genes (log2FC ≤ −1.5; adjusted *p*-value ≤ 0.05) comparing polysome and total genes sets for each differentiation. Tables indicate the top five terms related to biological processes. Rank of the term was based at *p*-value for neuroectoderm and combined score (EnrichR) for mesoderm and endoderm

these genes played a significant role during the differentiation process. For this analysis, we applied a threshold of Log2FC ≥ |1| with an adjusted *p*-value ≤ 0.05 to classify a gene as enriched or depleted in the polysome fraction (Fig. 5). Marked differences were observed between the germ layers. In endoderm samples, approximately 450 genes were depleted from and 460 genes were recruited to the polysomes. GO analysis revealed that the depleted genes were associated with processes such as extracellular matrix and structural organization, while the recruited genes were involved in nucleic acid and DNA-templated regulation.

In mesoderm samples, the differences between transcriptome and translatome were less pronounced, with only 22 genes recruited to polysomes. However, a considerable number of genes (209) were depleted from polysomes. Interestingly, GO analysis of the depleted genes highlighted processes similar to those observed in the endoderm, including regulation of extracellular matrix organization and integrin pathways. In the neuroectoderm, 176 genes were depleted from the translation machinery, while 130 genes were recruited to polysomes. GO analysis showed that the depleted genes were enriched for processes related to translation, such as "Cytoplasmic Translation", "Translation", and "Peptide Biosynthetic Process". In contrast, the polysome-recruited genes were associated with processes involving post-translational modifications (PTMs), such as "Regulation of Histone Modification", "Positive Regulation of Protein K63-linked Ubiquitination", and "Positive Regulation of Protein Polyubiquitination", although the number of genes representing each term was limited in this analysis. The list of genes identified as recruited to and depleted from polysome were available in Additional Table 4.

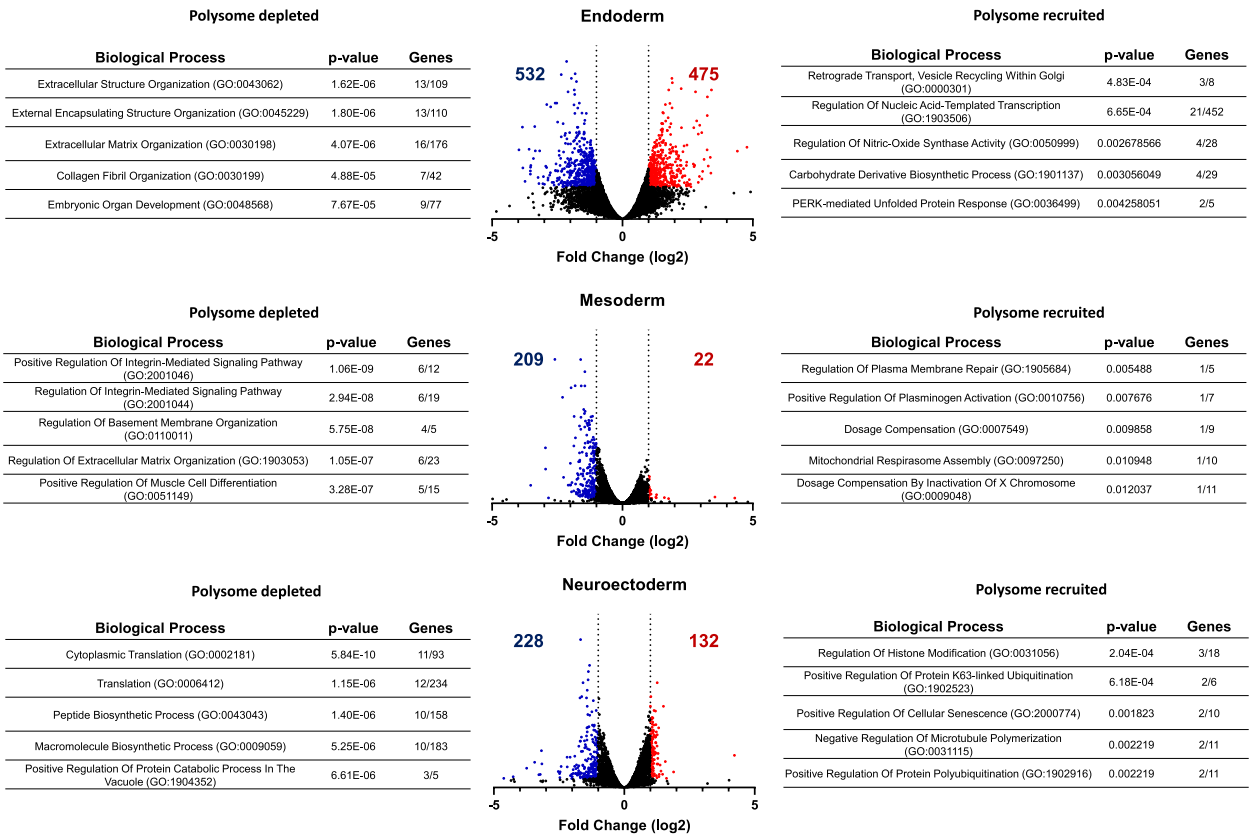

Fig. 5 Transcriptome and translatome comparison. Volcano plots for each differentiation protocol display the comparison between Total RNA (transcriptome) and Polysome-bound RNA (translatome). The Y-axis represents the adjusted *p*-value, while the X-axis represents the log2 fold change (threshold = |1|). Blue dots indicate genes depleted from polysomes, red dots indicate genes recruited to polysomes, and black dots represent genes with a log2 fold change ≤ |1| and/or an adjusted *p*-value > 0.05. The number of genes identified as depleted or recruited to polysomes is displayed within each volcano plot. The Gene Ontology tables show the biological processes associated with the identified genes: the table on the right highlights processes for genes recruited to polysomes, while the table on the left lists processes for genes depleted from polysomes. Terms are ranked by *p*-value using EnrichR

Discussion

During development, specific genes are expressed in distinct cells, contributing to the establishment of cellular diversity within an organism [30]. The gene expression program adheres to the central dogma of molecular biology, wherein proteins are synthesized based on the genetic information encoded in DNA, which is transcribed into RNA molecules. However, it has been demonstrated that there is a low correlation between the detection of mRNA and the actual presence of corresponding proteins [31–34]. Analyzing mRNA alone may not accurately reflect protein levels, making it less robust than approaches that consider translational regulation alongside gene transcription [35]. Therefore, the scientific community has discussed the analysis of the translatome instead of the transcriptome to recapitulate the ultimate gene expression [34–36]. To distinguish transcripts actively being translated into proteins, a viable method is to specifically target the RNA associated with cytoplasmic ribosomes. The polysome profiling technique offers a robust method to achieve this distinction [17, 37, 38].

Here, we submitted a hESC cell line to three germ layer differentiation processes and compared transcriptome and translatome data. Our analysis revealed a pervasive presence of post-transcriptional regulation in all three embryonic layer differentiation. Additionally, our findings demonstrate that analyzing translatome samples can unveil previously undetected genes whether analyzed only transcriptome. RNA-seq analysis of both polysome-bound and total RNA provided insights into potential differences between transcriptional and translational regulations. Interestingly, polysome-bound and total RNA datasets showed similar distribution of DEGs. However, comparison of the genes between both datasets revealed that a substantial number of genes undergo dynamic regulation during differentiation. Our findings align with previous studies demonstrating dynamic changes in gene recruitment to the translational machinery throughout development models and differentiation processes [36, 39]. While specific genes being regulated varied between differentiation protocols, the consistent proportion of regulatory events across all embryonic layers suggests a shared mechanism. This data addresses our question into whether the post-transcriptional regulation previously identified in mesoderm is a unique characteristic of this particular developmental lineage or a broader phenomenon across commitment processes of embryonic germ layers [13].

It is also worth emphasizing the significance of the translatome in understanding the buffering mechanisms that maintain the stability of protein levels, ensuring a specific phenotype despite significant fluctuations in mRNA levels. This phenomenon has been extensively studied in recent years and accounts for the phenotypic diversity observed among species, individuals of the same species, and different tissues within the same individual [40]. In our study, we demonstrate that, during the commitment of the three embryonic germ layers, translational regulation is present in these processes, similar to what has been shown for other cellular signaling pathways involved in developmental processes [41].

The comparison between transcriptome and translatome datasets has gained increasing interest in the recent years, prompting further exploration [42–44]. It is known that protein synthesis is a major regulator of gene expression during differentiation processes [45]; therefore, the translatome has been used to identify genes that impact these processes [35]. In our analysis of GO using datasets from the transcriptome and translatome of each differentiation group, we observed that the translatome either includes a higher number of terms related to the specific process or scores higher for those terms. This evidence indicates that the translatome dataset can accurately describe the process compared to the transcriptome dataset, as supported by the fact that all genes involved in the process overlap between both the total and polysome RNA fractions.

While these GO terms generally reflect expected differentiation pathways, some annotations may not fully align with the classical germ layer fates. This is a known limitation of GO term analysis, as certain genes, such as GATA4, which has been linked to both cardiac development and endoderm specification [27, 46, 47], or EOMES, which has been described in both endoderm and mesoderm [29, 48]. Therefore, in our analysis of the endoderm and mesoderm—two layers with very similar expression profiles—we used a combined score to group terms. It has been reported that distinguishing between these two layers during the early stages of differentiation is challenging due to their similar cell types and gene expression profiles, often referred to as endomesoderm or mesendoderm in the literature [49–51]. In line with this observation, in our gene set enrichment analysis (GSEA), performed to validate our differentiated datasets, we identified terms like 'Embryonic Skeletal System Development' in the neuroectoderm. This is likely due to the expression of HOX genes, which are known to regulate both neural and skeletal development [52]. While the skeletal system is primarily mesodermal in origin, certain transcription factors involved in its development are also expressed in ectoderm-related structures, such as the apical ectodermal ridge [53].

Finally, we compared the transcriptome and translatome profiles across each germ layer. This analysis revealed the complexity of post-transcriptional regulation in establishing germ layer identity, demonstrating distinct

patterns of gene recruitment to, and depletion from, polysomes. In the endoderm and mesoderm, we observed a pronounced depletion of genes associated with cell–matrix formation and interaction, suggesting a functional reprogramming that prioritizes intracellular processes over cell–matrix communication. The extracellular matrix (ECM) is known to play a crucial role in development by anchoring cells, shaping tissue architecture, and influencing cell migration [54, 55]. Our findings indicate that genes involved in these processes are targets of PTR in this model, highlighting the dynamic control of ECM-related pathways after the differentiation. In contrast, the neuroectoderm displayed depletion of genes associated with cytoplasmic translation and recruitment of genes involved in PTMs. This regulatory strategy suggests a reliance on PTMs to fine-tune the activity of key proteins in the neuroectoderm, consistent with prior studies emphasizing the critical role of PTMs in neural lineage specification and function [56, 57]. Collectively, these results demonstrated the PTR as a mechanism that is differentially orchestrated across germ layers to ensure their proper specification and functionality.

Overall, it is evident that studying the translatome is a key strategy for effectively and robustly mapping previously unknown gene expression programs involved in development and cellular commitment. Some authors assert that translational regulation is the most crucial step in the processing of genetic information [58].

Conclusions

Our findings reveal a substantial post-transcriptional modulation during germ layer commitment. Our analysis identified genes involved in germ layer differentiation that were not apparent in the transcriptome, emphasizing the robustness of polysome profiling for uncovering post-transcriptional regulation. These data highlight the presence of post-transcriptional mechanisms in early embryonic development, offering new perspectives on the molecular underpinnings of cell differentiation and supporting future studies on the functions of the genes identified during differentiation.

Abbreviations

DEG	differentially expressed genes
DHFR2	Dihydrofolate Reductase 2
DLX3	Distal-less Homeobox 3
DNA	deoxyribonucleic acid
FC	fold change
GFP	green fluorescent protein
GSEA	gene set enrichment analysis
GO	Gene Ontology
hESC	human embryonic stem cell
Log2FC	log_2 fold change
mRNA	messenger ribonucleic acid
PTR	post-transcriptional regulation
PTNR	post-transcriptional negative regulation
PTPR	post-transcriptional positive regulation
qPCR	quantitative polymerase chain reaction
RNA	ribonucleic acid
SD	standard deviation
UNC13D	Unc-13 Homolog D

Supplementary Information

The online version contains supplementary material available at https://doi.org/10.1186/s12864-025-11400-8.

Additional file 1: Table 1: The lists of genes identified as being regulated by PTR in Endoderm present in Fig. 3.

Additional file 2: Table 2: The lists of genes identified as being regulated by PTR in Mesoderm present in Fig. 3.

Additional file 3: Table 3: The lists of genes identified as being regulated by PTR in Neuroectoderm present in Fig. 3.

Additional file 4: Table 4: List of genes identified recruited to and depleted from polysome fraction. The criteria for genes been include were presented log2 fold change $\geq |1|$ and p-adjusted ≤ 0.05.

Additional file 5. Supplementary Table 1. List of primers used in qPCR.

Additional file 6. Figure S1. Characterization of polysome profiling and RNA sequencing data set. A. Representative polysome profiling charts for endoderm, mesoderm, and neuroectoderm cells. Y-axis represents RNA detection, while the X-axis corresponds to the fractions isolate by sucrose gradient. Polysome fractions was indicated in the figure. B. PCA plot generated from RNA-seq data obtained from total RNA samples (transcriptome). C. PCA plot generated from RNA-seq data obtained from polysome-bound RNA samples (translatome). D. Heatmap of RNA-seq data comparing total and polysome-bound RNA across the three germ layer commitments with no filter. Values are presented as counts per million (CPM). The color key legend is displayed next to the chart. E. PCA plot comparing transcriptome and translatome data for each sample.

Additional file 7. Figure S2. Validation of polysome-bound RNA identified in RNAseq. A-B. Representative polysome profiling of neuroectoderm after treatment with cycloheximide (A) and puromycin (B). C. qPCR analysis of DLX3, UNC13D and DHFR2 distribution in polysome profiling fractions. Mean with SD; Student's unpaired t-test analysis: ** $p < 0.01$.

Additional file 8. Figure S3. Gene ontology analysis of common DEGs. Gene ontology analysis using the up- (log2FC $\geq$ 1.5; adjusted p-value $\leq$ 0.05) and down-regulated (log2FC $\leq$ -1.5; adjusted p-value $\leq$ 0.05) genes common for the three germ layers, comparing polysome and total samples. Table indicates the top five terms related to biological processes. Rank of the term was based on p-value.

Acknowledgements

We would like to thank all the staff of the Carlos Chagas Institute (FIOCRUZ-PR) for the laboratory and administrative support. We also would like to thanks Program for Technological Development in Tools for Health (RPT-FIOCRUZ) for using the Genomic facility at Instituto Oswaldo Cruz – Fiocruz/RJ and qPCR facility at Instituto Carlos Chagas – Fiocruz/PR.

Authors' contributions

R.G.J. and C.D.S.H. developed the study concept, experimental design, performed experiments, analyzed the data and wrote the main manuscript text. I.T.P. performed experiments. A.F.F.H. and L.S. performed bioinformatic analysis. A.L.R. performed experiments and wrote the main manuscript text. B.D. developed the study concept, experimental design and supervised the project.

Funding

This work was financially supported by CNPq PROEP/ICC grant 442353/2019–7, INCT-REGENERA grant 88887.136364/2017–00. R.G.J. and C.D.S.H. received fellowships from FIOCRUZ and I.T.P, A.F.F.H. and A.L.R. from CAPES. B.D. received fellowship from CNPq.

Data availability
The datasets generated and analysed during the current study are available in the National Center for Biotechnology Information (NCBI) repository, accessing number PRJNA1144790.

Declarations

Ethics approval and consent to participate
Not applicable.

Competing interests
The authors declare no competing interests.

Author details
[1]Stem Cells Basic Biology Laboratory, Instituto Carlos Chagas - FIOCRUZ-PR, Curitiba 81.350-010, Brazil. [2]Bioinformatics Unit, Institut Pasteur de Montevideo, Montevideo, CP 11400, Uruguay. [3]Basic Medicine Department, Facultad de Medicina, Clinical Hospital, Universidad de La República Uruguay, Montevideo, CP 11100, Uruguay.

Received: 13 August 2024 Accepted: 24 February 2025
Published online: 08 March 2025

References

1. Ghimire S, Mantziou V, Moris N, Martinez AA. Human gastrulation: the embryo and its models. Dev Biol. 2021;474:100–8.
2. Semi K, Takashima Y. Pluripotent stem cells for the study of early human embryology. Dev Growth Differ. 2021;63:104–15.
3. Murry CE, Keller G. Differentiation of embryonic stem cells to clinically relevant populations: lessons from embryonic development. Cell. 2008;132:661–80.
4. Huang L, Li F, Ye L, Yu F, Wang C. Epigenetic regulation of embryonic ectoderm development in stem cell differentiation and transformation during ontogenesis. Cell Prolif. 2023;56:e13413.
5. Thomson M, Liu SJ, Zou L-N, Smith Z, Meissner A, Ramanathan S. Pluripotency factors in embryonic stem cells regulate differentiation into germ layers. Cell. 2011;145:875–89.
6. van Mierlo G, Wester RA, Marks H. A mass spectrometry survey of chromatin-associated proteins in pluripotency and early lineage commitment. Proteomics. 2019;19:1900047.
7. Semrau S, Goldmann JE, Soumillon M, Mikkelsen TS, Jaenisch R, van Oudenaarden A. Dynamics of lineage commitment revealed by single-cell transcriptomics of differentiating embryonic stem cells. Nat Commun. 2017;8:1096.
8. Lin Y, Li X-Y, Willis AL, Liu C, Chen G, Weiss SJ. Snail1-dependent control of embryonic stem cell pluripotency and lineage commitment. Nat Commun. 2014;5:3070.
9. Zhao BS, Roundtree IA, He C. Post-transcriptional gene regulation by mRNA modifications. Nat Rev Mol Cell Biol. 2017;18:31–42.
10. Li L, Miu K-K, Gu S, Cheung H-H, Chan W-Y. Comparison of multi-lineage differentiation of hiPSCs reveals novel miRNAs that regulate lineage specification. Sci Rep. 2018;8:9630.
11. Rad SMAH, Mohammadi-Sangcheshmeh A, Bamdad T, Langroudi L, Atashi A, Lotfinia M, et al. Pluripotency crossroads: junction of transcription factors, epigenetic mechanisms, MicroRNAs, and long non-coding RNAs. Curr Stem Cell Res Ther. 2017;12:300–11.
12. Li M, Izpisua Belmonte JC. Deconstructing the pluripotency gene regulatory network. Nat Cell Biol. 2018;20:382–92.
13. Pereira IT, Spangenberg L, Robert AW, Amorín R, Stimamiglio MA, Naya H, et al. Cardiomyogenic differentiation is fine-tuned by differential mRNA association with polysomes. BMC Genomics. 2019;20:1–16.
14. Caruso M, Meurant S, Detraux D, Mathieu A, Gilson M, Dieu M, et al. The global downregulation of protein synthesis observed during hepatogenic maturation is associated with a decrease in TOP mRNA translation. Stem Cell Rep. 2023;18:254–68.
15. Yan Y, Shin S, Jha BS, Liu Q, Sheng J, Li F, et al. Efficient and rapid derivation of primitive neural stem cells and generation of brain subtype neurons from human pluripotent stem cells. Stem Cells Transl Med. 2013;2:862–70.
16. Lian X, Zhang J, Azarin SM, Zhu K, Hazeltine LB, Bao X, et al. Directed cardiomyocyte differentiation from human pluripotent stem cells by modulating Wnt/β-catenin signaling under fully defined conditions. Nat Protoc. 2013;8:162–75.
17. Gomes-Júnior R, Shigunov P, Dallagiovanna B, Pereira IT. Accessing the human pluripotent stem cell translatome by polysome profiling. In: Turksen K. (eds) Embryonic Stem Cell Protocols. Methods in molecular biology, vol 2520. Humana, New York, NY. 2021. https://doi.org/10.1007/7651_2021_437.
18. Krueger F, Andrews SR, Osborne CS. Large scale loss of data in low-diversity illumina sequencing libraries can be recovered by deferred cluster calling. PLoS ONE. 2011;6:e16607.
19. Kim D, Langmead B, Salzberg SL. HISAT: a fast spliced aligner with low memory requirements. Nat Methods. 2015;12:357–60.
20. Anders S, Pyl PT, Huber W. HTSeq—a Python framework to work with high-throughput sequencing data. Bioinformatics. 2015;31:166–9.
21. Love MI, Huber W, Anders S. Moderated estimation of fold change and dispersion for RNA-seq data with DESeq2. Genome Biol. 2014;15:550.
22. Chen EY, Tan CM, Kou Y, Duan Q, Wang Z, Meirelles GV, et al. Enrichr: interactive and collaborative HTML5 gene list enrichment analysis tool. BMC Bioinformatics. 2013;14:128.
23. Fonseka P, Pathan M, Chitti SV, Kang T, Mathivanan S. FunRich enables enrichment analysis of OMICs datasets. J Mol Biol. 2021;433:166747.
24. Narita Y, Rijli FM. Chapter 5 hox genes in neural patterning and circuit formation in the mouse hindbrain. 2009:139–67.
25. Cho JH, Tsai MJ. The role of BETA2/NeuroD1 in the development of the nervous system. Mol Neurobiol. 2004;30:035–48.
26. Hans S, Liu D, Westerfield M. Pax8 and Pax2a function synergistically in otic specification, downstream of the Foxi1 and Dlx3b transcription factors. Development. 2004;131:5091–102.
27. Xuan S, Sussel L. GATA4 and GATA6 regulate pancreatic endoderm identity through inhibition of hedgehog signaling. Development. 2016;143:780–6.
28. Alexander J, Stainier DYR. A molecular pathway leading to endoderm formation in zebrafish. Curr Biol. 1999;9:1147–57.
29. Yi CH, Terrett JA, Li QY, Ellington K, Packham EA, Armstrong-Buisseret L, et al. Identification, mapping, and phylogenomic analysis of four new human members of the T-box gene family:EOMES, TBX6, TBX18, andTBX19. Genomics. 1999;55:10–20.
30. Cramer P. Organization and regulation of gene transcription. Nature. 2019;573:45–54.
31. Maier T, Güell M, Serrano L. Correlation of mRNA and protein in complex biological samples. FEBS Lett. 2009;583:3966–73.
32. King HA, Gerber AP. Translatome profiling: methods for genome-scale analysis of mRNA translation. Brief Funct Genomics. 2014. https://doi.org/10.1093/bfgp/elu045.
33. Chua BA, Van Der Werf I, Jamieson C, Signer RAJ. Post-transcriptional regulation of homeostatic, stressed, and malignant stem cells. Cell Stem Cell. 2020;26:138–59.
34. Wang Z-Y, Leushkin E, Liechti A, Ovchinnikova S, Mößinger K, Brüning T, et al. Transcriptome and translatome co-evolution in mammals. Nature. 2020;588:642–7.
35. Zhang JG, Xu C, Zhang L, Zhu W, Shen H, Deng HW. Identify gene expression pattern change at transcriptional and post-transcriptional levels. Transcription. 2019;10:137–46.
36. Hu W, Zeng H, Shi Y, Zhou C, Huang J, Jia L, et al. Single-cell transcriptome and translatome dual-omics reveals potential mechanisms of human oocyte maturation. Nat Commun. 2022;13:5114.
37. Pringle ES, McCormick C, Cheng Z. Polysome profiling analysis of mRNA and associated proteins engaged in translation. Curr Protoc Mol Biol. 2019;125:e79.
38. Holmes MJ, Misra J, Wek RC. Analysis of translational control in the integrated stress response by polysome profiling. 2022:157–71.
39. Samuels TJ, Gui J, Gebert D, Karam TF. Two distinct waves of transcriptome and translatome changes drive Drosophila germline stem cell differentiation. EMBO J. 2024;43:1591–617.
40. Buccitelli C, Selbach M. mRNAs, proteins and the emerging principles of gene expression control. Nat Rev Genet. 2020;21:630–44.

41. Fujii K, Shi Z, Zhulyn O, Denans N, Barna M. Pervasive translational regulation of the cell signalling circuitry underlies mammalian development. Nat Commun. 2017;8:14443.
42. Tebaldi T, Re A, Viero G, Pegoretti I, Passerini A, Blanzieri E, et al. Widespread uncoupling between transcriptome and translatome variations after a stimulus in mammalian cells. BMC Genomics. 2012;13:220.
43. van Heesch S, Witte F, Schneider-Lunitz V, Schulz JF, Adami E, Faber AB, et al. The translational landscape of the human heart. Cell. 2019;178:242-260.e29.
44. Imai H, Utsumi D, Torihara H, Takahashi K, Kuroyanagi H, Yamashita A. Simultaneous measurement of nascent transcriptome and translatome using 4-thiouridine metabolic RNA labeling and translating ribosome affinity purification. Nucleic Acids Res. 2023;51:e76–e76.
45. Kristensen AR, Gsponer J, Foster LJ. Protein synthesis rate is the predominant regulator of protein expression during differentiation. Mol Syst Biol. 2013;9:689.
46. Rojas A, Schachterle W, Xu SM, Martín F, Black BL. Direct transcriptional regulation of Gata4 during early endoderm specification is controlled by FoxA2 binding to an intronic enhancer. Dev Biol. 2010;346:346–55.
47. Zhou P, He A, Pu WT. Regulation of GATA4 transcriptional activity in cardiovascular development and disease. 2012:143–69.
48. Schröder CM, Zissel L, Mersiowsky S-L, Tekman M, Probst S, Schüle KM, et al. EOMES establishes mesoderm and endoderm differentiation potential through SWI/SNF-mediated global enhancer remodeling. Dev Cell. 2024. https://doi.org/10.1016/j.devcel.2024.11.014.
49. Sladitschek HL, Neveu PA. A gene regulatory network controls the balance between mesendoderm and ectoderm at pluripotency exit. Mol Syst Biol. 2019;15:e9043.
50. Han L, Chaturvedi P, Kishimoto K, Koike H, Nasr T, Iwasawa K, et al. Single cell transcriptomics identifies a signaling network coordinating endoderm and mesoderm diversification during foregut organogenesis. Nat Commun. 2020;11:4158.
51. McClay DR, Croce JC, Warner JF. Conditional specification of endomesoderm. Cells Dev. 2021;167:203716.
52. Feng W, Li Y, Kratsios P. Emerging roles for hox proteins in the last steps of neuronal development in worms, flies, and mice. Front Neurosci. 2022;15:801791.
53. Zakany J, Duboule D. The role of Hox genes during vertebrate limb development. Curr Opin Genet Dev. 2007;17:359–66.
54. Walma DAC, Yamada KM. The extracellular matrix in development. Development. 2020;147:dev175596.
55. Acloque H, Adams MS, Fishwick K, Bronner-Fraser M, Nieto MA. Epithelial-mesenchymal transitions: the importance of changing cell state in development and disease. J Clin Investig. 2009;119:1438–49.
56. Smith BJ, Carregari VC. Post-translational modifications during brain development. 2022:29–38.
57. Gupta R, Sahu M, Srivastava D, Tiwari S, Ambasta RK, Kumar P. Post-translational modifications: regulators of neurodegenerative proteinopathies. Ageing Res Rev. 2021;68:101336.
58. Zhao J, Qin B, Nikolay R, Spahn CMT, Zhang G. Translatomics: the global view of translation. Int J Mol Sci. 2019;20:212.

Publisher's Note